

# Pumping-field induced dynamic effects in micron-sized Permalloy lines and their influence on HF filter applications

T. Korn\*, M. Kerekes, U. Ebels

URA 2512 SPINTEC, CEA-CNRS, CEA-Grenoble, Bat 1005, 17 Av des Martyrs, 38054 Grenoble, France

\*email: korn@drfmc.ceng.cea.fr

D.Stanescu, P. Xavier

IMEP, UMR5130, CNRS-INPG-UJF, 23 Avenue des Martyrs, 38016 Grenoble, France

**Abstract**— We present a combined time- and frequency domain study on the dynamic properties of Permalloy (Py) lines with different shape anisotropies on top of coplanar waveguides. The observed results are compared to numerical simulations of the magnetization dynamics using a macrospin model. For small-angle excitation, the inductive measurement of the resonance frequency in the frequency domain is equal to that in the time domain. However, if high pumping field amplitudes are used in the time-domain measurements, additional effects appear that shift the resonance frequency. They are caused by the large precession angle of the magnetization and the tilting of the equilibrium angle of the magnetization due to the presence of the pumping field. Depending on whether the shape anisotropy of the Py line is larger or smaller than the pumping field, the direction of this shift is either to higher or to lower frequencies. The simulations qualitatively confirm these experimental observations.

## I. INTRODUCTION

In recent years, there has been a growing interest in miniaturized microwave devices for mobile communications and sensor applications. Ferromagnetic microstructures embedded in coplanar waveguides (CPWs) or other high-bandwidth transmission lines are currently being considered for high frequency filter applications [1]. Due to their high saturation magnetization, they can operate at higher frequencies than the ferrites that are currently used [2]. As standard process techniques (optical lithography, sputtering, dry etching) are used for their fabrication, they can easily be added to integrated circuits.

## II. SAMPLE PREPARATION AND EXPERIMENT

The coplanar waveguides have a total length of 5 mm. They taper to an inner conductor width of  $2.8 \mu\text{m}$  for a length of  $100 \mu\text{m}$ . They are fabricated by ion milling from a (50 nm Cu/5 nm Ta)<sub>5</sub> Pt 2 nm multilayer on a high-resistivity Si substrate. The Py lines are  $2 \mu\text{m}$  wide and  $100 \mu\text{m}$  long and are deposited on the inner conductor by optical lithography, magnetron sputtering of the Py layer and subsequent liftoff. The CPWs are contacted using high-bandwidth picoprobes. Time-domain experiments are performed with a pulsed inductive microwave magnetometer (PIMM) [3] consisting of a pulse generator capable of 10 V, 65 ps risetime pulses and a sampling oscilloscope with a bandwidth of 20 GHz.

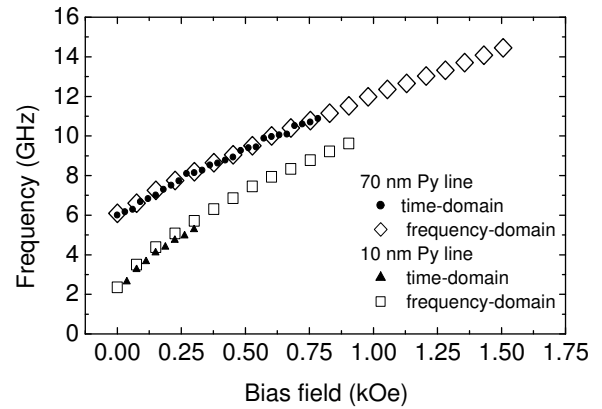


Fig. 1. Time- and frequency-domain dispersion for 70 nm and the 10 nm Py line.

Attenuators are used after the pulse has passed the CPW to protect the oscilloscope. Two perpendicular magnetic fields in the sample plane allow us to align the magnetization of the sample parallel ( $y$  direction) or perpendicular ( $x$  direction) to the pumping field created above the CPW to perform difference measurements and extract the inductive response of the sample. The time-domain response is further analyzed by performing a numerical fast fourier transformation (FFT) using a Hamming window function and zero padding. In the corresponding macrospin simulations, a numeric differentiation of the calculated  $y$ -component of the magnetization is performed to compare the result to the time derivative  $\frac{dM_y}{dt}$  which is proportional to the signal measured by the PIMM [3]. Frequency domain measurements are performed using a network analyzer with a bandwidth of 20 GHz. Here, the real part of the S12 transmission parameter is measured in the two different field configurations to determine the absorption due to ferromagnetic resonance within the sample. This technique has been used in recent years to determine the dynamic properties of ferromagnetic microstructures like lines [4] and rings [5], as well as thin films [6]. To compare the frequency-domain measurements to macrospin calculations, the experiment was modelled in the following way: a sinusoidal pumping field

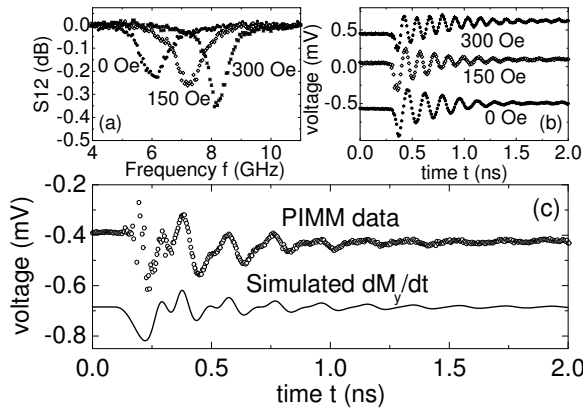


Fig. 2. (a) Frequency domain data for 70 nm thick Py line for different bias fields. (b) Low-excitation PIMM data for 70 nm thick Py line. (c) High-excitation (10 V pulse) PIMM data and corresponding macrospin simulation for the 10 nm thick Py line. The PIMM trace was taken at  $H_{Bias} = 75$  Oe. For the simulated  $\frac{dM_y}{dt}$ , the same bias field and  $H_{Pulse} = 370$  Oe were used.

of variable frequency is used to drive the macrospin. The steady-state oscillation amplitude is determined as a function of the excitation frequency. The oscillation amplitude has its maximum at the ferromagnetic resonance frequency.

### III. RESULTS

Figure 2 (a) and (b) show typical frequency and time domain data obtained for the 70 nm thick Py line. From these data, the resonance frequencies are extracted from the maximum of the absorption (frequency domain) and the maximum of the FFT (time domain). For small excitation amplitudes, the resonance frequencies as a function of bias field determined by frequency and time domain measurements match closely, as Figure 1 shows. The shape anisotropy of the Py lines is extracted by fitting the Kittel formula  $f_r = |\gamma|/(2\pi)\sqrt{(H_{Bias} + H_{ani})(M_S + H_{Bias} + H_{ani})}$ , where  $H_{ani}$  is the uniaxial in-plane anisotropy field and  $\gamma = 176$  GHz/Tesla is the gyromagnetic ratio, to the resonance frequency as a function of the bias field. Here, we obtain  $H_{ani}(10 \text{ nm}) = 61$  Oe for the 10 nm thick line and  $H_{ani}(70 \text{ nm}) = 370$  Oe for the 70 nm thick line. As higher pulse amplitudes (up to 10 V) are used in the PIMM experiment, a field pulse amplitude  $H_{Pulse}$  of about 300 Oe is created above the CPW - the pulse duration of 10 ns is longer than the relaxation time of the magnetization. We observe two effects of this high field pulse amplitude:

- 1) For zero or low bias fields, the PIMM traces for both lines show a pronounced deviation from a damped sine behavior, the oscillation becomes nonharmonic and the frequency changes from  $2f$  to  $f$  as it dampens out (figure 2 (c)).
- 2) At moderate and high bias fields, the resonance frequency of the oscillation shifts by up to 1.3 GHz as a function of the pulse amplitude. The direction of this shift is different for the 10 nm and the 70 nm line, as figure 3 (a) and (b) show.

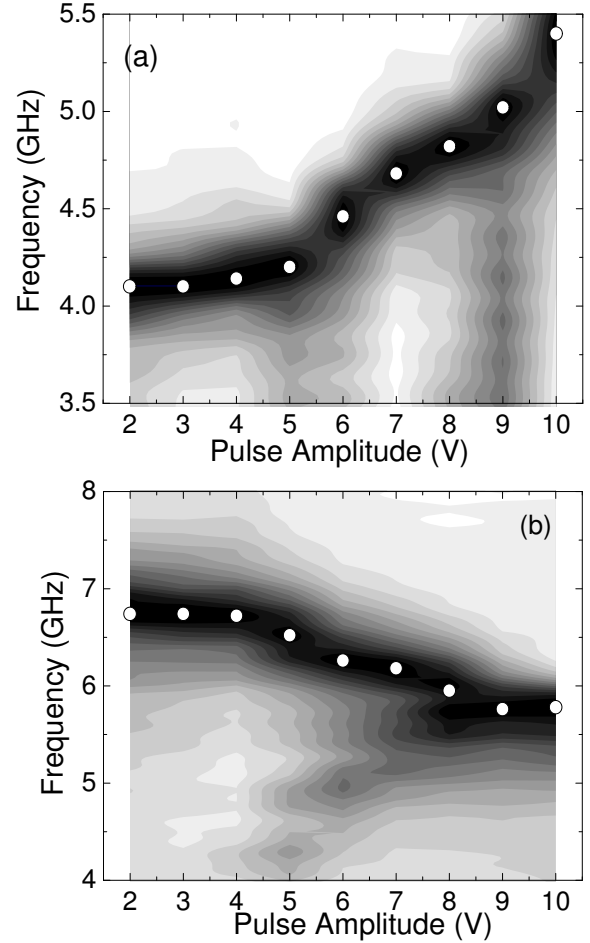


Fig. 3. Greyscale plots: FFT of the PIMM data as function of pulse amplitude for  $H_{Bias} = 150$  Oe: (a) 10 nm thick Py line, (b) 70 nm thick Py line. The resonance peaks are marked by white circles.

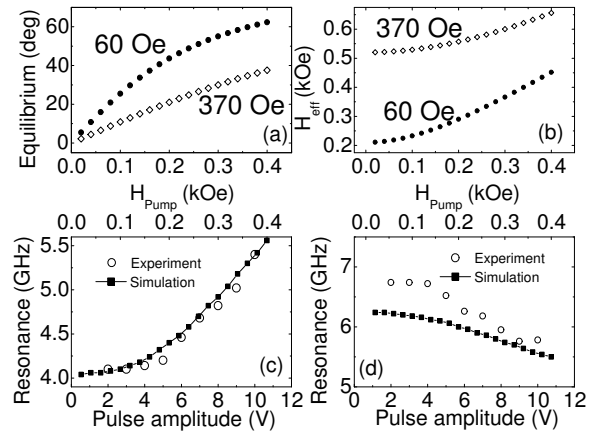


Fig. 4. Calculations for  $H_{Bias} = 150$  Oe: (a) In-plane equilibrium angle as function of  $H_{Pulse}$ . (b) Total effective field as function of  $H_{Pulse}$ . Measured resonance frequencies compared to values extracted from macrospin calculations for  $H_{Bias} = 150$  Oe: (c) 10 nm thick Py line, (d) 70 nm thick Py line.

The first effect is caused by the high excitation angle of the magnetization due to the fast-rising field pulse. It can be described in the macrospin model if a high damping value  $\alpha = 0.2$  is used, as the calculated derivative of  $M_y$  in figure 2 (c) shows.

The second effect is caused by the quasi-DC component of the field pulse which changes the effective field. The equilibrium angle of the magnetization is thus changed: it is no longer parallel to the easy axis, along which the bias field is applied, but tilted parallel to the effective field according to the vector sum  $\vec{H}_{eff} = \vec{H}_{Bias} + \vec{H}_{Ani} + \vec{H}_{Pulse}$ . The observed frequency shift is also described in the macrospin model, as figure 4 (c) and (d) demonstrates. For the moderate bias field applied, both the simulation of the time-domain experiment and a frequency-domain simulation using a small-angle forced oscillation around  $\vec{H}_{eff}$  yield the same resonance frequencies.

Figure 4 (b) shows the calculated amplitude of  $\vec{H}_{eff}$  for the different values of  $H_{Ani}$ . We distinguish two cases:

- $H_{Ani} < H_{Pulse}$   
Here, the increased amplitude of the effective field due to  $H_{Pulse}$  causes an increase of the resonance frequency. As the calculation in figure 4 (b) shows for the 10 nm Py line, the amplitude of  $\vec{H}_{eff}$  more than doubles in the accessible range of  $H_{Pulse}$ .
- $H_{Ani} \approx H_{Pulse}$   
Here,  $H_{Pulse}$  tilts the magnetization towards the hard axis of the sample resulting in a decrease of the resonance frequency. In the range of  $H_{Pulse}$  examined in figure 4(b), the amplitude of  $\vec{H}_{eff}$  increases only about 25 percent, so the influence of shape anisotropy dominates the change of resonance frequency.

#### IV. FAST TUNABLE FILTER APPLICATIONS

As Figure 1 shows, the attainable damping for the 70 nm thick line is about 0.4 dB, corresponding to  $40 \frac{\text{dB}}{\text{cm}}$ . Even larger values can be reached if a thicker Permalloy layer is used [2]. Using shape anisotropy the operating frequency of the filter can be tailored to the range required by the application. It may also serve to reduce the effective damping in the ferromagnetic structure [7] and increase the quality factor. The frequency shift effect caused by the tilting of the equilibrium direction of the magnetization can be exploited to create a fast tunable notch filter. The quasi-DC current needed to shift the resonance frequency can either be combined with the microwave signal by using a Bias-T element, or a separate current line can be deposited on top of the coplanar waveguide. The tuning range of the filter is mainly limited by the DC resistivity of the current line, as excessive heating and electromigration may destroy it. In order to avoid large excursion angles of the magnetization before it stabilizes around its new equilibrium as seen in Figure 2, the risetime of the quasi-DC-current should be larger than 1 over the resonance frequency. However, this still allows for a modulation of the notch filter resonance frequency at 1 GHz or more, a value that would be impossible to obtain if an externally created bias field were used for tuning.

#### V. SUMMARY

We have performed time- and frequency resolved measurements of the magnetization dynamics of microstructured Py lines with different shape anisotropies. For small-angle excitations of the magnetization, the observed resonance frequencies match closely and allow us to determine the value of the shape anisotropy. As high pump field amplitudes are used in the time-domain measurements, we observe nonlinear oscillations of the magnetization for low applied bias fields. For moderate bias fields, the pump field causes a shifting of the resonance frequency. The direction of this shift depends on the ratio of shape anisotropy and pump field: for low shape anisotropy, the pump field serves mainly to increase the amplitude of the effective field, thus increasing the resonance frequency. For higher shape anisotropy, the pump field tilts the magnetization towards its hard axis, thus reducing the resonance frequency. This effect may be used in tunable notch filters for microwave frequencies to modulate the operating frequency of the filter at 1 GHz or more.

#### ACKNOWLEDGMENTS

The authors would like to thank J.P. Nozieres for his continuous support and Th. Fournier for access to Nanofab2000. M. Kerekes and T. Korn gratefully acknowledge financial support by the European Union via Research Training Network "ULTRASPIN".

#### REFERENCES

- [1] B. Kuanr, L. Malkinski, R. E. Camley, Z. Celinski and P. Kabos, J.Appl. Phys. 93, 8591 (2003)
- [2] B. Kuanr, Z. Celinski and R. E. Camley, Appl. Phys. Lett. 83, 3969 (2003)
- [3] T.J. Silva, C.S. Lee, T.M. Crawford and C.T. Rogers, J.Appl. Phys. 85, 7849 (1999)
- [4] M. Kerekes, A. D. C. Viegas, D. Stanescu, P. Xavier, G. Suran and U. Ebels, J.Appl. Phys. 95, 6616 (2004)
- [5] F. Giesen et al., submitted to J.Appl. Phys. (2005)
- [6] S. Kaka, J. P. Nibarger, S. E. Russek, N. A. Stutzke and S. L. Burkett, J.Appl. Phys. 93, 7539 (2003)
- [7] T. Korn, F. Giesen, J. Podbielski, D. Ravlic, C. Schueller and D. Grundler, J. Magn. Mater. 285, 240 (2005)